



DEVELOPMENT OF AN IN SITU SYSTEM AND ANALYSIS PROCEDURE FOR MEASURING GROUND THERMAL PROPERTIES

Abdeen Mustafa Omer

Energy Research Institute (ERI), Nottingham, UK

Abstract: Globally buildings are responsible for approximately 40% of the total world annual energy consumption. Most of this energy is for the provision of lighting, heating, cooling and air conditioning. An increase in awareness of the environmental impact of CO₂, NO_x and CFCs emissions triggered a renewed interest in environmentally friendly cooling and heating technologies. Under the 1997 Montreal Protocol, governments agreed to phase out chemicals used as refrigerants that have the potential to destroy stratospheric ozone. It was therefore considered desirable to reduce energy consumption in order to decrease the rate of depletion of world energy reserves as well as the pollution to the environment. One way of reducing building energy consumption is to design buildings, which are more efficient in their use of energy for heating, lighting, cooling and ventilation. Passive measures, particularly natural or hybrid ventilation rather than air-conditioning, can dramatically reduce primary energy consumption. Therefore, promoting innovative renewable energy applications including the ground source energy may contribute to preservation of the ecosystem by reducing emissions at local and global levels. This will also contribute to the amelioration of environmental conditions by replacing conventional fuels with renewable energies that produce no air pollution or the greenhouse gases (GHGs). An approach is needed to integrate renewable energies in a way to achieve high building performance standards. However, because renewable energy sources are stochastic and geographically diffuse, their ability to match demand is determined by the adoption of one of the following two approaches: the utilisation of a capture area greater than that occupied by the community to be supplied, or the reduction of the community's energy demands to a level commensurate with the locally available renewable resources. Ground source heat pump (GSHP) systems (also referred to as geothermal heat pump systems, earth-energy systems and GeoExchange systems) have received considerable attention in recent decades as an alternative energy source for residential and commercial space heating and cooling applications. The GSHP applications are one of three categories of geothermal energy resources as defined by ASHRAE and include high-temperature (>150°C) for electric power production, intermediate temperature (<150°C) for direct-use applications and GSHP applications (generally (<32°C)). The GSHP applications are distinguished from the others by the fact that they operate at relatively low temperatures.

Keywords: Renewable energy technology, ground source heat pump, built environment

NOMENCLATURE

c_p specific heat, J/kg K

H borehole depth, m

K slope, dimensionless

L probe length, m

m flow rate, kg/m³

q heat transfer rate per unit depth, W/m

t temperature, °C

UI heating power, W

Greek

λ thermal conductivity, W/m K

η calibration factor, dimensionless

τ heating time, s

Academic Journal of Current Research

An official Publication of Center for International Research Development

Double Blind Peer and Editorial Review International Referred Journal; Globally index

Available www.cird.online/AJCR; E-mail: AJCR@CIRD.ONLINE



Subscript

<i>in</i>	inlet
<i>out</i>	outlet
<i>f</i>	average
<i>HP</i>	heat pump
<i>HDPE</i>	high-density polyethylene
<i>wi</i>	inlet of the HP units

1. INTRODUCTION

In recent years, ground source heat pumps (GSHPs) have been used increasingly for space heating and air-conditioning of buildings and for the purpose of energy saving and emission reduction (Sanner, Karytsas, Mendrinis, and Rybach, 2003; Omer, 2008). In these systems, borehole heat exchangers (BHEs) are usually used to exchange heat with the underground environment. It is accepted that heat conduction is the predominant mechanism for heat transfer of the BHEs in most saturated fine-grained soils. Previous studies have shown that backfill materials have a certain influence on the thermal performance of the BHEs (Gu, Dennis, 1998; Cote, Konrad, 2005; Chehaba, Moore, 2010). Generally, the increase in the thermal conductivity of backfill materials is helpful to reduce the thermal resistance between the BHEs and the surrounding soils, which was expected to be a major approach to shortening the required length of the BHEs for the GSHP applications.

Thermally enhanced backfill materials, therefore, have been paid much attention by researchers and designers during the past decade. For example, Allan (Allan, 2000) tested the mean thermal conductivity of sand-cement grouts in the saturated state, ranging from 2.49 W/m K at laboratory to 2.19 W/m K in field tests. By adding ballast material into bentonite, Engelhardt and Finsterle (Engelhardt, Finsterle, 2003) obtained a high thermal conductivity of 2.3 to 2.6 W/m K, leading to an increase in heat conduction. Li, et al. (Li, Chen, Chen,

Zhao, 2006) compared the effects of sandstone and cement backfills on the thermal performances of two vertical BHEs in a cold climate region. Wang, et al. (Wang, Ma, Huang, Gong, 2007) developed a super absorption polymer mixed with the original soil as backfilled material of the BHEs. Qi, et al. (Qi, Wang, Wang, 2010) compared the thermal performance of the BHEs with saturated medium-coarse sand and fine sand as backfill materials, where a 6-10% enhancement on heat transfer was obtained. More recently, due to a good water absorbing and swelling property of bentonite crystals, sand-bentonite mixtures are used frequently as a backfill material for vertical boreholes in many GSHP applications, which are also recommended by (ASHRAE, 2007). However, selection of backfill materials for geothermal boreholes is a complex function of thermal, regulatory, and economic considerations (Omer, 2012). There are still some problems to be solved, such as the effect of the mixed ratio, saturation, grain sizes and other factors on the thermal conductivity of sand-bentonite mixtures, which finally may influence the thermal performance of the BHEs.

The objective of this communication was to quantitatively analyse the effects of sand-bentonite backfill materials on the thermal performance of the BHEs. Thermal needle probe tests were conducted at laboratory to measure the thermal conductivity of sand-bentonite mixtures in order to seek for an optimal mixed ratio. Based on microscopic observations, the mechanism of bentonite affecting heat conduction between the sand grains was analysed. Further, field tests were carried out to compare the thermal performance of two BHEs with an optimal sand-bentonite mixture and a common medium-coarse sand mixture as backfill materials, respectively. The present study can provide helpful guides for the design of the GSHP systems.

2. EXPERIMENTAL STUDY

This study is an introduction to the energy problem and the possible saving that can be achieved through



improving building performance and the use of ground energy sources. The relevance and importance of the study is discussed in the communication, which, also, highlights the objectives of the study, and the scope of the theme.

2.1. Laboratory Experiments

In this study, thermal probe tests (TPTs) were performed to measure the thermal conductivity of sand-bentonite backfill materials. TPT is a typical laboratory unsteady analysis method, in which the thermal conductivity of porous media is obtained by the temperature increase of an infinite constant linear heat source within an infinite object (Waite, Gilbert, Winters, 2006). Carslaw and Jaeger (Carslaw, Jaeger, 1964) proposed an analytical representation for this problem. An approximated solution of analytical representation can be written as follows (Bristow, White, and Kluitenberg, 1994):

$$\lambda = \eta \frac{UI}{4\pi kL}$$

Where UI is the heating power, L is the probe length, η is the calibration factor, and k is the slope of the intermediate linear part of the curve of the temperature rise Δt versus the logarithmic time $\ln(\tau)$.

As shown in Figure 1, a 140 mm long stainless steel pipe with the outer diameter of 2.0 mm was used as a thermal needle probe. The enamel-insulated constantan wires with the diameter of 0.1 mm and the resistance of 35 to 40 ohm were used as a linear heat source and heated electrically by a WYJ-15 type DC power meter with a constant voltage output ranging from 5 to 10 V. The wires were carefully installed into the probe. At the same time, a copper-constantan temperature sensor with $\pm 0.1^\circ\text{C}$ accuracy was installed at the half length of the probe. Before the installation, the sensor was calibrated carefully. Finally, in order to reduce the response time, the probe was filled with the silicone grease with metal powders. Usually, the aspect ratio (length: diameter) of

needle probes should be higher than 55 to obtain idealised conditions of an infinite linear heat source which is required to fulfill the thermal probe theoretical assumptions. The deviation from this assumption can be compensated by using the factor η . In the present work, the commercial glycerol with a purity of over 99% was used as a standard sample (0.286 W/m K at 20°C) to calibrate the TPT results (Wang, Liu, Qi, 2010). After calibration, the maximum test error was about $\pm 2\%$. Prior to the TPTs, the probe was inserted vertically into a sample. After 5 min, a constant heating power was applied. Simultaneously, an Aglient-34970 A type data acquisition recorder was used to record the variations of the needle probe temperature during the tests. The heating time for each test was about five to eight minutes.

Two types of sand, i.e., fine sand (0.1-0.3 mm) and coarse sand (0.5-0.8 mm), were chosen by the screen sizer for the preparation of matrix samples. Commercially available sodium bentonite with 86% montmorillonite was used as the additive, and its average ratio of water absorption was 300% (after 2h). After measurement, the dry density of sand and bentonite were 1580 kg/m^3 and 1460 kg/m^3 , respectively. Figure 2 shows the micrographs of dry sand and bentonite, which were obtained by a SIGE300-type optical microscope. It can be seen that the average diameter of bentonite powders was by far smaller than that of sand. Therefore, once tiny bentonite powders are mixed fully with fine or coarse sand, they will be able to take up the pores surrounded by those relatively large sand grains, thereby influencing the heat conduction capability of the whole mixture.

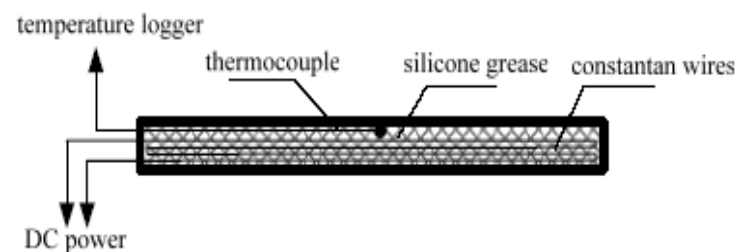




Figure 1. Diagram of a thermal needle probe measuring the thermal conductivity of porous media.

For the preparation of sand-bentonite mixtures, both sand and bentonite were placed into a dry box at 105°C. After drying for 12 h, the samples were cooled down to the room temperature. Then, sand and bentonite were fully mixed according to different ratios of dry weight. Further, pure water with a certain mass was added into the sand-bentonite mixtures, mixed fully to reach a required saturation and then moved into different sealed metal cylinders with the diameter of 110 mm and the height of 240 mm. After 2 h, the cylinders were uncovered to conduct the TPTs at room temperature.

2.2. Field Tests

For the GSHP applications, the heat transfer rate of a BHE as a function of depth can be calculated by the measured inlet and outlet fluid temperature and the flow rate through the BHE. It can be expressed as

$$q = mc_p (t_{in} - t_{out}) / H$$

where q is the heat transfer rate per unit depth, m is the flow rate, c_p is specific heat, t_{in} and t_{out} are the inlet and outlet fluid temperature of the BHE, respectively, and H is the borehole depth.



Figure 2. Micrographs of dry sand and bentonite grains.

Figure 3 shows the experimental setup testing the thermal performance of a BHE. The setup mainly consisted of a heat/cold source system, a measuring system, and a vertical BHE. The heat/cold source system was able to keep a relatively constant temperature inside a 40 L insulated water tank, thus guaranteeing a stable inlet fluid temperature to the BHE. The water tank was made

of stainless steel plates. The stainless steel plates were 2 mm thick, and the polyurethane insulation layer surrounding them was 30 mm thick. The heating was provided by an adjustable electric water heater, while the cooling was obtained by means of a typical R22 refrigeration cycle consisting of a Daikin-JT95 type rotor compressor, a fin condenser, an expansion valve, and a coil evaporator. The condenser was cooled by an axial air-cooling fan. The maximum heating and cooling output was 12 kW and 9 kW, respectively. In addition, an advanced proportional-integral-derivative (PID) temperature controller was mounted on the operation panel. The operation temperature for the water tank ranged from 5 to 40°C, with the accuracy of $\pm 0.5^\circ\text{C}$. A 90 W Wiley-RS25 type circulating pump was used to keep the flow circuit. Its maximum flow rate and the hydraulic head were 2.5 m³/h and 6 m, respectively.

The measuring system included two Pt1000-type temperature sensors with $\pm 0.1^\circ\text{C}$ accuracy, a GPR-II type electromagnetic flow meter with $\pm 0.001\text{m}^3/\text{h}$ accuracy. Before the installation, all temperature sensors were calibrated by an XLR-1 type constant-temperature bath with $\pm 0.01^\circ\text{C}$ accuracy.

For comparison, the thermal performance of two double U-shaped BHEs with different backfill materials was tested in Figure 4 shows a part of view of field tests. The BHEs were made of high-density polyethylene materials. The depth and diameter of both boreholes were 105 m and 200 mm, respectively. The distance between two boreholes was 15 m. For backfill materials, one borehole was grouted by unsized sand containing a little of clay, and another by the sand-bentonite mixture. The mixed ratio of the latter was determined by the results of laboratory measurements, which will be discussed in the following sections. In addition, all exposed pipes were insulated effectively using black polyethylene foam materials with a thickness of 20 mm, in order to reduce the undesired loss of heat or cold. Other more details on the experimental setup can be seen in our previous studies



(Wang, Qi, Gu, Du, 2009). Data collection was once every 10 minutes, and the test period extended from 10 September to 30 September 2010.

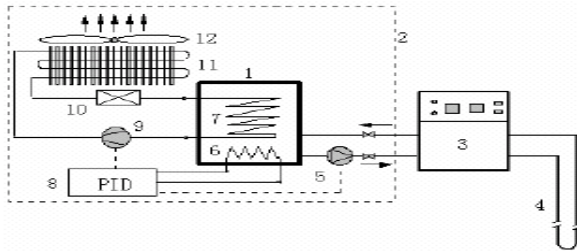


Figure 3. Diagram of the experimental setup testing the thermal performance of a BHE.

Figure 5 shows the laboratory results of the thermal conductivity of sand-bentonite mixtures with different mixed ratios under the saturation of 80%. It can be seen that the thermal conductivity of sand-bentonite mixtures first increases with increasing percentage of bentonite by dry mass, then reaches a peak at a certain percentage range, beyond which the thermal conductivity decreases. In detail, the optimal percentage of bentonite by dry mass as backfill materials of the BHEs was 10% for the fine sand-bentonite mixture and 12% for the coarse sand-bentonite mixture, and the corresponding thermal conductivity was 2.15 W/m K and 2.37 W/m K, which were 36.1% and 26.7% higher than that of fine sand and coarse sand at the same saturation, respectively. Note that when the percentage of bentonite exceeded 15%, the thermal conductivity decreased gradually and finally reached the value of about 0.75 W/m K, which was in good agreement with the thermal conductivity of saturated bentonite recommended by (ASHRAE, 2007 and Villar, et al., 1996). Therefore, the measurement results of the TPTs in this study were reliable. During the experiments, we also found that, as the saturations of sand-bentonite mixtures were over 80%, they were no longer be compacted because little compressible air remain and only low compressible water was left.



Figure 4. A part of view of field tests of the thermal performance of the BHEs Results and Discussion.

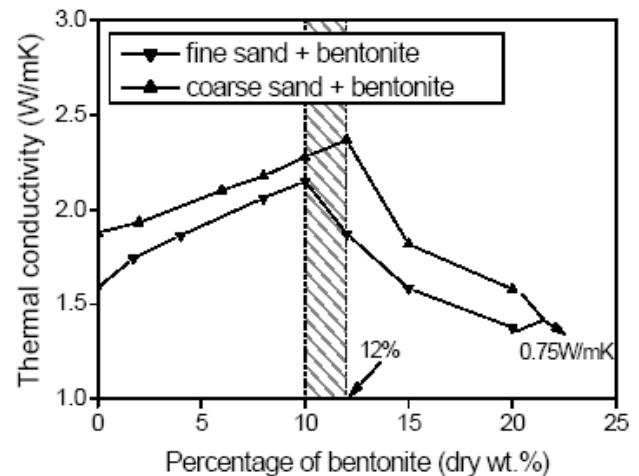


Figure 5. Thermal conductivities of sand-bentonite mixtures with different mixed ratios.

It should be noted that ASHRAE also recommended the thermal conductivity ranges of three types of sand-bentonite mixtures as follows: i) 2.08 to 2.42 W/m K for 10 wt. % bentonite and 90 wt. % sand, ii) 1.00 to 1.10 W/m K for 15 wt. % bentonite and 85 wt. % sand, iii) 1.47 to 1.64 W/m K for 20 wt. % bentonite and 80 wt. % sand (ASHRAE, 2007). By contrast with the measurement results in this study, it is clear that there was a good agreement for the first and third situation, exception for the second case that was not confirmed in our study. So the present laboratory measurements extended the results recommended by ASHRAE.



From the point of view of microscopic observations shown in Figure 6, the enhancement mechanism of bentonite on the thermal conductivity of sand-bentonite mixtures can be explained as follows: when bentonite is added into sand, it will absorb water and swell quickly due to the hydrophilicity of montmorillonite mineral crystals, and finally become a sticky paste taking up those local or whole pores surrounding the sand grains. Thus, heat conduction between the solid grains is enhanced greatly by a higher thermal conductivity of bentonite, e.g., 0.75 W/m K at saturations of over 75 to 80%, than that of water (0.6 W/m K at 20°C). On the other hand, with continually increasing percentage of bentonite, the amount of sand tends to decrease and most sand grains are surrounded by the bentonite paste with a lower thermal conductivity than that of quartz (7.7 W/m K) and other minerals (2-3 W/m K depending on the quartz content of the total sand solids) (Hiraiwa, Kasubuchi, 2000; Ochsner, Horton, Ren, 2001; Lu, Ren, Gong, 2007), thereby resulting in a weakening of heat conduction between the solid grains. Henceforth, for sand-bentonite mixtures used as a backfill material of geothermal boreholes, there exists an optimal percentage of bentonite by dry mass, i.e., 10-12%, as shown in the shadow region of Figure 5. If the requirements on the thermal performance of the BHEs are not very strict, an extended range of 8-12% wt. bentonite is acceptable, too. Further, the mixture of 90% wt. medium and coarse sand and 10% wt. bentonite was determined in the field tests as an optimal backfill material to compare the thermal performance of the BHE. Firstly, in order to obtain the natural ground temperature, the BHE was operating under the condition without heating or cooling, only driven by the circulating pump. As shown in Figure 7, the inlet and outlet fluid temperature reached a steady state after 12 h. According to the recommendation by the International Energy Agency (IEA), the natural ground temperature is usually treated as the average fluid temperature at the above steady state. In the present study, this temperature

was calculated as 17.3°C after 16 h measurement. In addition, it should be noted that the natural ground temperature has a seasonal effect, which is mainly caused by the seasonal variations of the ground temperature at the shallow zone reaching a depth of about 2-20 m. If so, the heat transfer performance of the BHE may be affected to a certain extent (Wang, Qi, Wang, 2008). Considering the test period in this study was not very long, however, the above seasonal effect was neglected.

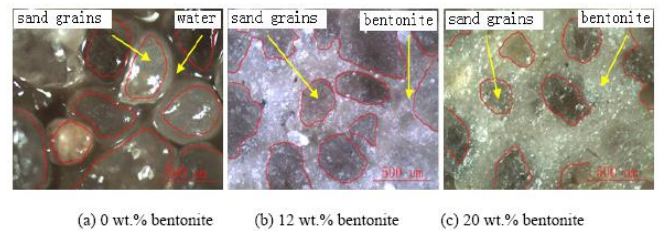


Figure 6. Micrographs of coarse sand-bentonite mixtures with different mixed ratios (80% saturation).

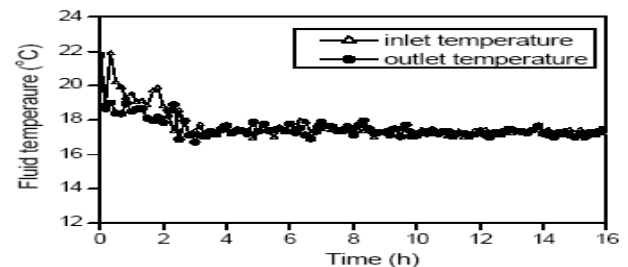


Figure 7. Test results of the natural ground temperature.

Secondly, two heat extraction and two heat injection experiments were performed in order to evaluate the thermal performance of each BHE and its surrounding soils. In each operation mode, the BHE was run at a succession of the inlet fluid temperatures, which further determined the fluid temperature t_{wi} entering the heat pump units. In fact, selecting the appropriate t_{wi} is critical in the design of the GSHP systems. Usually, choosing a value close to the natural ground temperature results in higher system efficiency, but makes the required length of the BHEs very long and thus unreasonably expensive. Choosing a value far from the natural ground temperature



allows selection of a small, inexpensive BHE, but the system's heat pumps will have greatly reduced capacity during heating and high demand when cooling.

According to the recommendation by (ASHRAE, 2007), t_{wi} should be 11 to 17°C higher than the ground temperature in cooling and 6 to 11°C lower than the ground temperature in heating, which is a good compromise between first cost and efficiency. In this study, the inlet fluid temperatures of the BHE were adjusted within the range from 6 to 9°C for heat extraction and from 28 to 32°C for heat injection, respectively.

Figure 8 and Figure 9 show two typical experimental results of the thermal performance of the BHE under a sand-clay and optimal sand-bentonite backfill material, respectively, where the average flow rate through the BHE was 1.05 m³/kg. It can be seen that, as the cooling time increased, the heat extraction rate of the BHE dropped gradually and then tended to be relatively steady after 24 to 30 h, and as the heating time increased, the heat injection rate of the BHE increased rapidly, and then dropped gradually to reach relatively steady after 20 to 24 h. Here, the positive and negative sign for the heat transfer rate of the BHEs only represent the direction of thermal energy injected into and extracted from the ground, respectively.

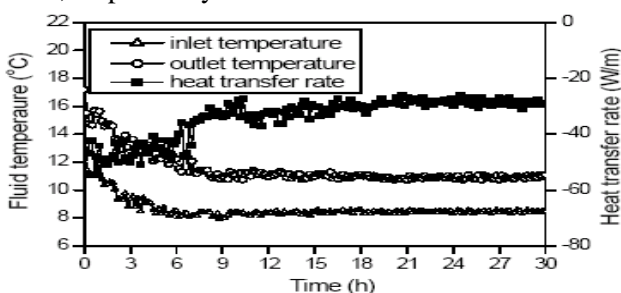


Figure 8. Thermal performances of the BHE with a common sand-clay backfill material.

It can also be seen by comparison that backfill materials had a great impact on the thermal performance of the BHEs. For example, for the heat extraction

operation mode, the heat transfer rate was (-29.6 W/m) at an average fluid temperature of 9.3°C under sand-clay backfilling and -35.5 W/m at an average fluid temperature of 9.5°C under sand-bentonite backfilling, respectively. For the heat injection operation mode, the heat transfer rate was 34.5 W/m at an average fluid temperature of 28.0°C under sand-clay backfilling and 38.3 W/m at an average fluid temperature of 26.8°C under sand-bentonite backfilling, respectively.

(a) Heat extraction (inlet fluid temperature: 8.4°C)

(b) Heat injection (inlet fluid temperature: 30.2°C)

Finally, Figure 10 shows the variations of the heat transfer rate of the BHE with the average fluid temperature. Through the regression using the Least Square Method, there appeared a clear linear relation, which further provided an important basis for evaluating the thermal performance of the BHE under different operation conditions. In detail, the heat transfer rate of the BHE in the field tests satisfied the following equations: 1)

$$q = 3.367t_f - 59.974 \text{ for sand-bentonite material, and 2)}$$

$$q = 4.273t_f - 74.498 \text{ for sand-clay material, where } t_f \text{ is}$$

the average fluid temperature and equals to $(t_{in} + t_{out}) / 2$.

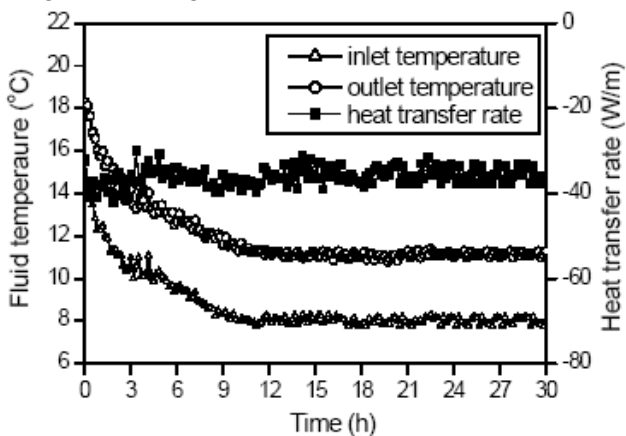
It can be easily seen that, compared with the case with a common sand-clay material, both the heat injection and heat extraction rate of the BHE with an optimal sand-bentonite backfill material were enhanced.

After calculation, for the range of the fluid temperature of 6 to 9°C for heat extraction and 28 to 32°C for heat injection, the enhancement on the heat transfer of the BHE was 22.2% and 31.1%, respectively. These results are helpful to greatly reduce the required length of the BHEs in the GSHP applications. (Allen, et al., 1997) also found a 22 to 37% reduction in the required length of the BHEs when cement-sand grouts with a thermal conductivity of (2.2 to 2.5 W/m K) were used as a backfill material. By contrast, I can draw on a preliminary conclusion that, for the sand-bentonite backfill material

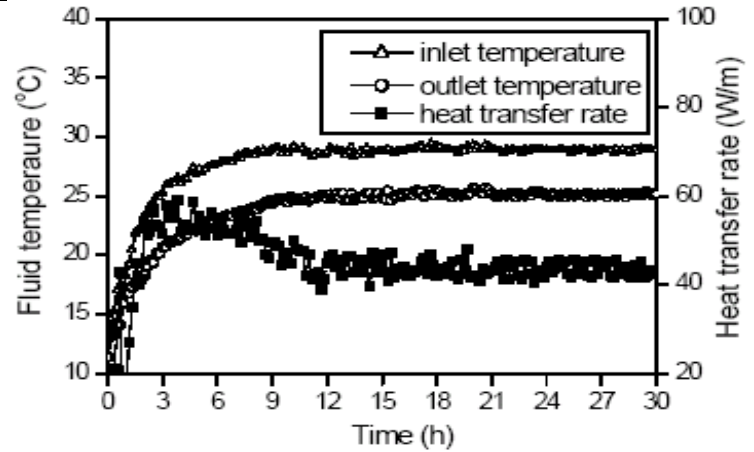


with a thermal conductivity higher than 2.14 W/m K, the reduction in the required length of the BHEs should be at least 20 percent, depending on the soil thermal conductivity and bore diameter, which in turn can be used as one of criteria for choosing backfill materials with a good thermal performance. Therefore, the above optimal sand-bentonite backfill material can be safely used for the construction of the BHEs in the GSHP systems.

The term “ground source heat pump” has become an inclusive term to describe a heat pump system that uses the earth, ground water, or surface water as a heat source and/or heat sink. The GSHPs utilise the thermal energy stored in the earth through either a vertical or horizontal closed loop heat exchangers buried in the ground. Many geological factors impact directly on site characterisation and subsequently the design and cost of the GSHP systems. The geological prognosis for a site and its anticipated rock properties influence the drilling methods and therefore the system cost (Abdeen Omer, 2009). Other factors that are important to system design include predicted subsurface temperatures and the thermal and hydrological properties of strata. The GSHP technology is well established in Sweden, Germany and North America, but has had minimal impact in the United Kingdom space heating and cooling market (Abdeen Omer, 2009).



(a) Heat extraction (inlet fluid temperature: 8.0 °C)



(b) Heat injection (inlet fluid temperature: 28.9 °C)

Figure 9. Thermal performances of the BHE with an optimal sand-bentonite backfill material.

3. OVERVIEW OF GROUND SOURCE HEAT PUMP SYSTEMS

The GSHPs utilise the thermal energy stored in the earth through either vertical or horizontal closed loop heat exchange systems buried in the ground. Many geological factors impact directly on site characterisation and subsequently the design and cost of the system. The solid geology of the United Kingdom varies significantly. Furthermore there is an extensive and variable rock head cover. The geological prognosis for a site and its anticipated rock properties influence the drilling methods and therefore system costs. Other factors important to system design include predicted subsurface temperatures and the thermal and hydrological properties of strata. The GSHP technology is well established in Sweden, Germany and North America, but has had minimal impact in the United Kingdom space heating and cooling market. Perceived barriers to uptake include geological uncertainty, concerns regarding performance and reliability, high capital costs and lack of infrastructure. System performance concerns relate mostly to uncertainty in design input parameters, especially the temperature and thermal properties of the source. These in turn can impact on the capital cost, much of which is associated with the



installation of the external loop in horizontal trenches or vertical boreholes. The temperate United Kingdom climate means that the potential for heating in winter and cooling in summer from a ground source is less certain owing to the temperature ranges being narrower than those encountered in continental climates. This project will develop an impartial GSHP function on the site to make available information and data on site-specific temperatures and key geotechnical characteristics.

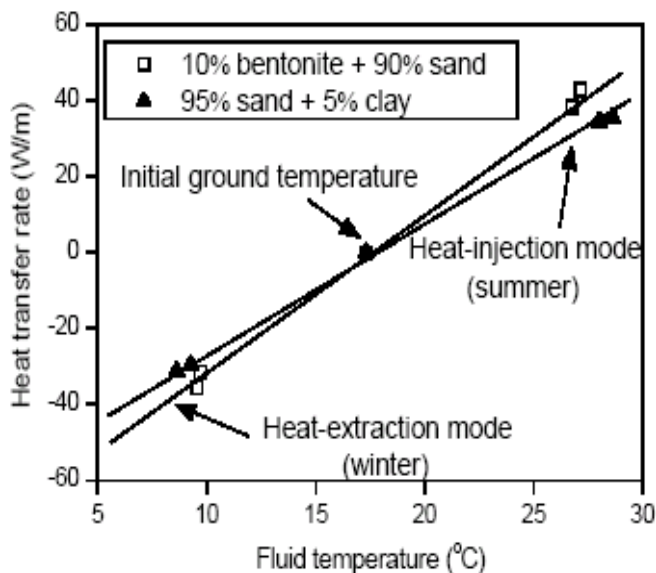


Figure 10. Variations of the heat transfer rate of the BHEs with average fluid temperatures.

The GSHPs are receiving increasing interest because of their potential to reduce primary energy consumption and thus reduce emissions of greenhouse gases. The technology is well established in North Americas and parts of Europe, but is at the demonstration stage in the United Kingdom. The information will be delivered from digital geoscience's themes that have been developed from observed data held in corporate records. These data will be available to the GSHP installers and designers to assist the design process, therefore reducing uncertainties. The research will also be used to help inform the public as to the potential benefits of this technology.

The GSHPs play a key role in geothermal development in Central and Northern Europe. With borehole heat exchangers as heat source, they offer decentral geothermal heating at virtually any location, with great flexibility to meet given demands. In the vast majority of systems, no space cooling is included, leaving ground-source heat pumps with some economic constraints. Nevertheless, a promising market development first occurred in Switzerland and Sweden, and now also is obvious in Austria and Germany. Approximately 20 years of research and development (R&D) focusing on borehole heat exchangers resulted in a well-established concept of sustainability for this technology, as well as in sound design and installation criteria. The market success brought Switzerland to the third rank worldwide in geothermal direct use. The future prospects are good, with an increasing range of applications including large systems with thermal energy storage for heating and cooling, ground-source heat pumps in densely populated development areas, borehole heat exchangers for cooling of telecommunication equipment, etc.

Efficiencies of the GSHP systems are much greater than conventional air-source heat pump systems. A higher COP (coefficient of performance) can be achieved by a GSHP because the source/sink earth temperature is relatively constant compared to air temperatures. Additionally, heat is absorbed and rejected through water, which is a more desirable heat transfer medium because of its relatively high heat capacity. The GSHP systems rely on the fact that, under normal geothermal gradients of about 0.5°F/100 ft (30 °C/km), the earth temperature is roughly constant in a zone extending from about 20 ft (6.1 m) deep to about 150 ft (45.7 m) deep. This constant temperature interval within the earth is the result of a complex interaction of heat fluxes from above (the sun and the atmosphere) and from below (the earth interior). As a result, the temperature of this interval within the earth is approximately equal to the average annual air



temperature (Abdeen Omer, 2010). Above this zone (less than about 20 feet (6.1 m) deep), the earth temperature is a damped version of the air temperature at the earth's surface. Below this zone (greater than about 150 ft (45.7 m) deep), the earth temperature begins to rise according to the natural geothermal gradient.

Abdeen (Abdeen Omer, 2010) groups GSHP systems into three categories based on the heat source/sink used. A fourth category is added here for the sake of completeness. These categories are: (1) ground-water heat pump (GWHP) systems, (2) ground-coupled heat pump (GCHP) systems, (3) surface water heat pump (SWHP) systems, and (4) standing column well (SCW) systems. Each of these is discussed in the following subsections.

3.1. Ground Water Heat Pump Systems

Ground water heat pump (GWHP) systems, also referred to as open-loop systems, are the original type of the GSHP system. The first GWHP systems were installed in the late 1940s (Abdeen Omer, 2011). The GWHP systems are not the focus of this thesis, so they will only be briefly described here. A schematic of a GWHP system is shown in Figure 11. In the GWHP systems, conventional water wells and well pumps are used to supply ground water to a heat pump or directly to some application. Corrosion protection of the heat pump may be necessary if ground water chemical quality is poor. The “used” ground water is typically discharged to a suitable receptor, such as back to an aquifer, to the unsaturated zone (as shown in Figure 11), to a surface-water body, or to a sewer.

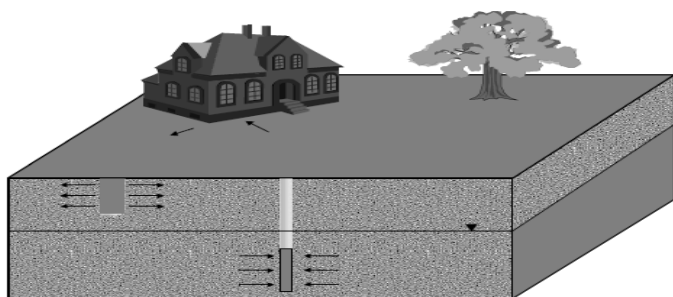


Figure 11. A schematic of a ground-water heat pump system.

Design considerations for the GWHP systems are fairly well established; well-drilling technologies and well-testing methods have been well known for decades. Design considerations include: ground-water availability, ground-water chemical quality, and ground-water disposal method. The main advantage of the GWHP systems is their low cost, simplicity, and small amount of ground area required relative to other GSHP and conventional systems. Disadvantages include limited availability and poor chemical quality of ground water in some regions. With growing environmental concerns over recent decades, many legal issues have arisen over ground water withdrawal and re-injection in some localities.

The direct expansion (DX) GSHP installed for this study was designed taking into account the local meteorological and geological conditions. The site was at the School of the Built Environment, University of Nottingham, where the demonstration and performance monitoring efforts were undertaken. The heat pump has been fitted and monitored for one-year period. The study involved development of a design and simulation tool for modelling the performance of the cooling system, which acts a supplemental heat rejecting system using a closed-loop GSHP system.

3.2. Ground Coupled Heat Pump Systems

Grounds coupled heat pump (GCHP) systems, also referred to as closed-loop ground-source heat pump systems, and were pioneered in the 1970s. Their main advantage over their water-well predecessors is that they eliminate the problems associated with ground water quality and availability and they generally require much less pumping energy than water well systems because there is less elevation head to overcome. The GCHP systems can be installed at any location where drilling or earth trenching is feasible. In GCHP systems, heat rejection/extraction is accomplished by circulating a heat exchange fluid through a piping system buried in the



earth. This fluid is either pure water or an antifreeze solution and is typically circulated through high-density polyethylene (HDPE) pipe installed in vertical boreholes or horizontal trenches as shown in Figure 12. Thus, these systems are further subdivided into vertical GCHP systems and horizontal GCHP systems.

3.3. Vertical Ground Coupled Heat Pump Systems

Vertical borehole GCHP systems are the primary focus of this entire thesis. Therefore, they are described in some detail here and their design challenges are explained, laying the foundation for the motivation of this study. In vertical borehole GCHP systems, ground heat exchanger configurations typically consist of one to tens of boreholes each containing a U-shaped pipe through which the heat exchange fluid is circulated. Some Swedish applications use boreholes inclined from the vertical. A number of borehole-to-borehole plumbing arrangements are possible. Typical U-tubes have a diameter in the range of $\frac{3}{4}$ in. (19 mm) to $1\frac{1}{2}$ in. (38 mm) and each borehole is typically 100 ft (30.5 m) to 300 ft (91.4 m) deep with a diameter ranging from 3 in. (76 mm) to 5 in. (127 mm). The borehole annulus is generally backfilled with a material that prevents contamination of ground water.

The design of vertical ground heat exchangers is complicated by the variety of geological formations and properties that affect their thermal performance (Abdeen Omer, 2012). Proper subsurface characterisation is not economically feasible for every project. One of the fundamental tasks in the design of a reliable GCHP system is properly sizing the ground-coupled heat exchanger length (i.e., depth of boreholes). Particularly for large systems, an extensive effort is made to design the ground loop heat exchangers so that they are not too large (resulting in too high of a first cost) or too small (resulting in the building's thermal load not being met).

In the early days of the GCHP technology, the task of sizing the ground-loop heat exchanger was accomplished using rules of thumb (i.e., 250 feet of bore length per ton

of heating or cooling capacity). These rules were slightly modified on a case-by-case basis using some estimates of thermal conductivity of the formation or using previous design experience, but additional costs of more detailed testing or calculations was judged to outweigh the costs of a conservative design. This relatively simple approach proved to be successful in most residential and other small applications, but in larger-scale commercial and institutional applications, some ground-loop heat exchangers failed to meet their design loads after the first few years of operation. Further, the practice of greatly over-designing large GCHP systems was found to be unacceptable because the first costs were simply not competitive with the first costs of conventional systems.

Consequently, intensive research regarding methods to optimise ground-loop heat exchanger design has been ongoing for the last decade. Simple approaches to sizing the ground-loop heat exchanger in larger-scale applications are inadequate mainly because the heat transfer processes in the ground are complicated by thermally interacting boreholes and hourly periodic heat extraction/injection pulses. Annual heat rejection and heat extraction are usually not equal and peak temperatures rise or fall over a number of years. As a result, ground-loop heat exchanger designers need to consider hourly heating and cooling loads of the building and need to perform some simulation of the ground-loop temperatures over the life-cycle of the building. Recent research efforts have produced several methods and computer software programmes for this purpose. However, none of the programmes consider the effects of ground water flow on ground-loop heat exchanger performance; these effects have not been well understood, perhaps because of the lack of relevant investigations.

Another challenge in the design of the GCHP systems arises from the fact that most commercial and institutional buildings, even in moderate climates, are generally cooling dominated and therefore reject more heat to the ground than they extract over the annual cycle.



This load imbalance may require the heat exchanger length to be significantly greater than the length required if the annual loads were balanced. As a result, the GSHP system may be eliminated from consideration early in the design phase of the project due to excessive first cost. This has given rise to the concept of “supplemental heat rejecters” or so-called “hybrid GSHP systems”.

Supplemental heat rejecters have been integrated into building designs to effectively balance the ground loads and therefore reduce the necessary length of the ground-loop heat exchanger. In some applications, the excess heat that would otherwise build up in the ground may be used for domestic hot water heaters, car washes, and pavement heating systems. In cases where the excess heat cannot be used beneficially, conventional cooling towers or shallow ponds can provide a cost-effective means to reduce heat exchanger length. Design of these supplemental components adds to the challenge of designing the overall hybrid GCHP system because of their highly transient nature. Heat rejection systems are likely to operate more often during the nighttime hours or when the building is not in use. Therefore, it is essential that the hourly (or less) behaviour of these systems be examined during their design phase.

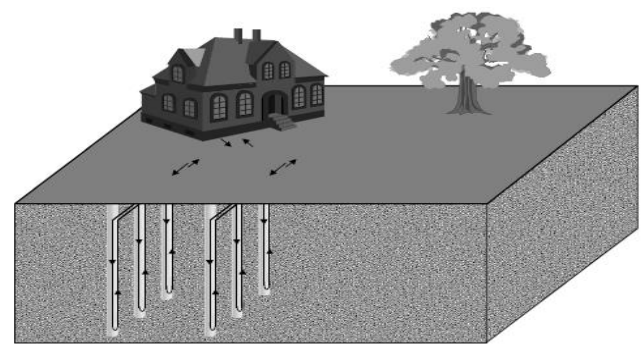
3.4. Horizontal Ground Coupled Heat Pump Systems

In horizontal GCHP systems, ground heat exchanger configurations typically consist of a series of parallel pipe arrangements laid out in dug trenches or horizontal boreholes about 3 ft (0.91 m) to 6 ft (1.83 m) deep. A number of piping arrangements are possible. “Slinky” configurations (as shown in Figure 12 (b)) are popular and simple to install in trenches and shallow excavations. In horizontal boreholes, straight pipe configurations are installed. Typical pipes have a diameter in the range of $\frac{3}{4}$ in. (19 mm) to 1 $\frac{1}{2}$ in. (38 mm) and about 400 ft (121.9 m) to 600 ft (182.9 m) of pipe is installed per ton of heating and cooling capacity.

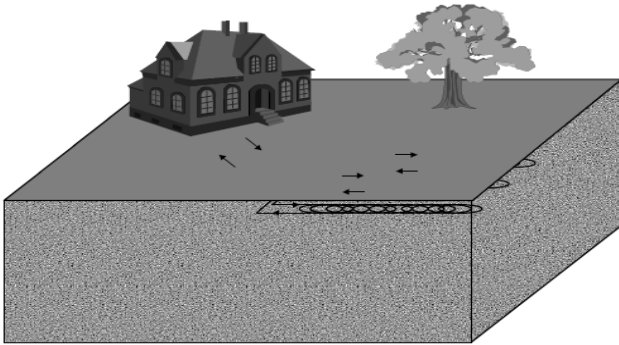
The thermal characteristics of horizontal GCHP systems are similar to those of vertical ones. The main

difference is that horizontal ground-loop heat exchangers are more affected by weather and air temperature fluctuations because of their proximity to the earth’s surface. This may result in larger loop temperature fluctuations and therefore lower heat pump efficiencies. Recent research activities have focused on using these systems as supplemental heat rejecters with vertical borehole GCHP systems. A specific application (i.e., the use of a shallow cooling system) is the focus of this study.

Aside from the invention of the slinky coil itself and the use of these systems as supplemental heat rejecters, horizontal systems have received much less attention than vertical systems with respect to recent research efforts. This may be due to the fact that vertical systems tend to be preferred in larger applications since much less ground area is required. Also, since horizontal systems are installed at shallow depths, geologic site characterisation is relatively easier because soils can be readily seen and sampled. Further, over-conservative designs are not as cost prohibitive as with vertical borehole designs because of the relatively low installation costs of the heat exchanger pipe.



(a)



(b)

Figure 12. A schematic of (a) A vertical borehole ground-coupled heat pump system and (b) Horizontal ground-coupled heat pump system.

3.5. Surface Water Heat Pump Systems

The third category of the GSHP systems is the surface-water heat pump (SWHP) system. A specific application of the SWHP systems (i.e., the use of a shallow pond as a supplemental heat rejecter in vertical GCHP systems), and a schematic of a SWHP system is shown in Figure 13. The surface-water heat exchanger can be a closed-loop or open-loop type. Typical closed-loop configurations are the Slinky coil type (as shown in Figure 14) or the loose bundle coil type. In the closed-loop systems, heat rejection/extraction is accomplished by circulating a heat exchange fluid through HDPE pipe positioned at an adequate depth within a lake, pond, reservoir, or other suitable open channel. Typical pipe diameters range from $\frac{3}{4}$ in. (19 mm) to $1\frac{1}{2}$ in. (38 mm) and a length of 100 feet (30.48 m) to 300 feet (91.44 m) per ton of heating or cooling capacity is recommended by Abdeen (Abdeen Omer, 2012), depending on the climate. In open-loop systems, water is extracted from the surface-water body through a screened intake area at an adequate depth and is discharged to a suitable receptor.

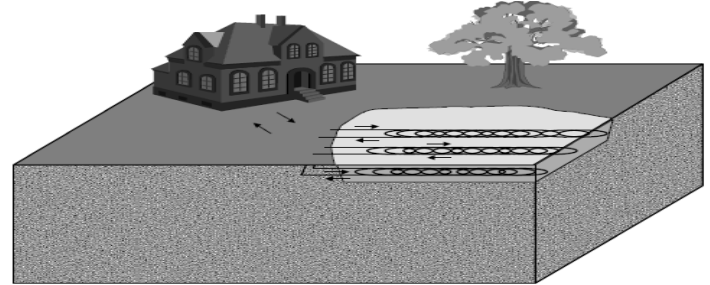


Figure 13. A schematic of a surface-water heat pump system.

Heat transfer mechanisms and the thermal characteristics of surface-water bodies are quite different than those of soils and rocks. At the present time, design tools for surface-water heat pump systems are in their developmental infancy (Abdeen Omer, 2012). However, many successful installations are currently in operation and some guidelines do exist. In short, the loop design involves selection of sufficient length of coil for heat transfer, specifying adequate diameter piping, specifying a sufficient numbers of parallel loops, and locating the coil at a proper depth in a water body with adequate thermal capacity.

3.6. Standing Column Well Systems

The fourth category of the GSHP systems is known as a standing column well (SCW) system. These systems are about as old as the ground-water heat pump systems, but are recently receiving much attention. Since these are not the subjects of this communication, they are only briefly discussed here.

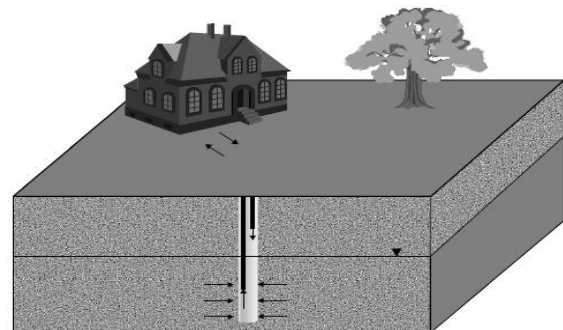




Figure 14. A schematic of a standing column well system.

A schematic of an SCW system is shown in Figure 14. This type of the GSHP draws water to a heat pump from a standing column of water in a deep well bore and returns the water to the same well. These systems, primarily installed in hard rock areas, use uncased boreholes with typical diameters of about 6 in. (15.24 cm) and depths up to 1500 feet (457.2 m). The uncased borehole allows the heat exchange fluid to be in direct contact with the earth (unlike closed-loop heat exchangers) and allows ground water infiltration over the entire length of the borehole. Properly sited and designed, SCW systems have been shown to have significant installation cost savings over closed-loop GSHP systems. Design guidelines for the SCW systems are currently under development.

4. SOIL PROPERTIES

One of the fundamental tasks in the design of a reliable ground source heat pump system is properly sizing the ground source heat exchanger length (i.e., depth of boreholes). Recent research efforts have produced several methods and commercially available design software tools for this purpose (Freeze, Witherspoon, 1967; Fetter, 1981; Isiorho, Meyer, 1999). These design tools are based on principles of heat conduction and rely on some estimate of the ground thermal conductivity and volumetric specific heat. These parameters are perhaps the most critical to the system design, yet adequately determining them is often the most difficult task in the design phase.

4.1. Groundwater Management

A further complication in the design of ground source heat pump systems is the presence of groundwater. Where groundwater is present, flow will occur in response to hydraulic gradients and the physical process affecting heat transfer in the ground is inherently a coupled one of heat diffusion (conduction) and heat advection by moving ground water. In general, groundwater flow can be expected to be beneficial to the thermal performance of

closed-loop ground heat exchangers since it will have a moderating effect on borehole temperatures in both heating and cooling modes.

4.2. Groundwater Flow

Underground water occurs in two zones: the unsaturated zone and the saturated zone. The term 'groundwater' refers to water in the saturated zone. The surface separating the saturated zone from the unsaturated zone is known as the 'water table'. At the water table, water in soil or rock pore spaces is at atmospheric pressure. In the saturated zone (below the water table), pores are fully saturated and water exists at pressures greater than atmospheric. In the unsaturated zone, pores are only partially saturated and the water exists under tension at pressures less than atmospheric. Groundwater is present nearly everywhere, but it is only available in usable quantities in aquifers. Aquifers are described as being either confined or unconfined. Unconfined aquifers are bounded at their upper surface by water table. Confined aquifers are bounded between two layers of lower permeability materials. In practice, the boreholes of ground-loop heat exchangers may partially penetrate several geologic layers.

The governing equation describing flow through porous media is Darcy's Law (Darcy, 1856):

$$q = S \, dh/dx$$

Where q is the specific discharge, (volume flow rate per unit of cross-sectional area), S is the hydraulic conductivity, and h is the hydraulic head. The specific discharge is related to average linear groundwater velocity, v , by:

$$v = q/n$$

Where n is the porosity and is introduced to account for the difference between the unit cross-sectional area and the area of the pore spaces through which the groundwater flows (Freeze, Cherry, 1989; Fetter, 1980). By applying the law of conservation of mass to a control volume and by making use of Darcy's Law (Eq. 3), an equation defining the hydraulic head distribution can be



derived. Transient groundwater flow with constant density can then be expressed in Cartesian tensor notation as:

$$S_s \frac{\partial h}{\partial t} - \frac{\partial}{\partial x_i} \left(K_{ij} \frac{\partial h}{\partial x_j} \right) = R^*$$

Since groundwater at 43.3°C (an extreme temperature limit expected in the GSHP applications) has a specific gravity of approximately 0.991, the assumption of constant density flow for low-temperature geothermal applications may be considered valid.

4.3. Heat Transport in Groundwater

Heat can be transported through a saturated porous medium by the following three processes:

- Heat transfer through the solid phase by conduction.
- Heat transfer through the liquid phase by conduction, and
- Heat transfer through the liquid phase by advection.

The governing equation describing mass or heat transport in groundwater is a partial differential equation of the advection-dispersion type (Freeze, Cherry, 1979). By applying the law of conservation of energy to a control volume, an equation for heat transport in groundwater can be found and can be expressed as:

$$nR \frac{\partial T}{\partial t} + v_i \frac{\partial T}{\partial x_i} - \frac{\partial}{\partial x_i} \left(D_{ij} \frac{\partial T}{\partial x_j} \right) = Q^*$$

where the velocity v_i is determined from the solution of Eq. 5 and T is the temperature of rock/water matrix. If the groundwater velocity is zero, Eq. 6 reduces to a form of Fourier's Law of heat conduction (Fournier, Potter, 1979; Fournier, Rowe, 1966; Fournier, Truesdell, 1959). The diffusion coefficient tensor D_{ij} is modelled as an effective thermal diffusivity given by:

$$D^* = k_{eff}/\rho_l C_l$$

The effective thermal conductivity k_{eff} is a volume-weighted average thermal conductivity of the saturated rock matrix and can be expressed using the porosity as:

$$k_{eff} = nk_l + (1-n)k_s$$

It is necessary to distinguish between the conductivity and thermal capacity of the water and soil/rock in this way to account for the fact that heat is stored and conducted through both the water and soil/rock, but heat is only advected by the water. Similarly, it is necessary to define a retardation coefficient R accounting for retardation of the thermal plume, which results from, differences in the liquid and solid volumetric heat capacities:

$$R = \frac{1 + (1-n)\rho_s C_s}{n\rho_l c_l}$$

Darcy's Law indicates that flow is dependent on both the local hydraulic gradient and the hydraulic conductivity of the geologic material. Heat transfer is dependent on the flow velocity and the thermal properties of the material. The thermal properties of soils and rocks are functions of mineral content, porosity and degree of saturation. Of these, porosity may be considered the most important property simply because of the origin and nature of soils and rocks. Rocks originate under higher heat and pressure environments than soils and consequently generally possess lower porosities.

4.4. Soil Thermal Measurements

The soil thermal measurements were carried out using KD2 Pro thermal properties analyser (Figure 15). The KD2 Pro is a handheld device used to measure thermal properties (Figure 16). The KD2 Pro is a battery-operated, menu-driven device that measures thermal conductivity and resistivity, volumetric specific heat capacity and thermal diffusivity. It consists of a handheld controller and sensors inserted into the medium to be measured (Figure 17). The single-needle sensors measure thermal conductivity and resistivity, while the dual-needle



sensor also measures volumetric specific heat capacity and diffusivity (Figures 18-20). Other types are summarised in appendix (1).

k is the thermal conductivity (W/m K)

R is the thermal resistivity (m K/W)

C is the specific heat capacity (MJ/m³ K)

D is the thermal diffusivity (mm²/s)

r is correlation coefficient

4.4.1. Specifications

KD2 Pro has been designed for ease of use and maximum functionality. Operating environment as follows:

Controller: 0-50°C

Sensors: -50 to +150°C

Battery life 1800 readings in constant use

Accuracy ±5

If the temperature of the sample medium is different from the temperature of the needle, the needle must equilibrate to the surrounding temperature before beginning a reading.

(Carslaw and Jaeger, 1959) modelled the temperature surrounding an infinite line heat source with constant heat output and zero mass in an infinite medium. When a quantity of heat Q (Jm⁻¹) is instantaneously applied to the line heat source, the temperature rise at distance r (m) from the source is:

$$\Delta T = \frac{Q}{4\pi kt} \exp\left(\frac{-r^2}{4Dt}\right)$$

where k is the thermal conductivity (W/m K), D is the thermal diffusivity (mm²/s) and t is time (s). If a constant amount of heat is applied to a zero mass heater over a period of time, rather than as an instantaneous pulse, the temperature response is:

$$\Delta T = \frac{q}{4\pi k} Ei\left(\frac{-r^2}{4Dt}\right) \begin{matrix} \text{During cooling } (t > t_1) \text{ it is:} \\ 0 < t \leq t_1 \end{matrix} \quad (11)$$

Where q is the rate of heat dissipation (W/m), t₁ is the heating time and Ei is the exponential integral (Abramowitz, Stegun, 1972). The temperature rise after the heat is turned off is given by:

$$\Delta T = \frac{q}{4\pi k} \left[-Ei\left(\frac{-r^2}{4Dt}\right) + Ei\left(\frac{-r^2}{4D(t-t_1)}\right) \right] t > t_1$$

Material thermal properties are determined by fitting the time series temperature data during heating to Eq. 11 and during cooling to Eq. 12. Thermal conductivity can be obtained from the temperature of the heated needle (single needle), with r taken as the radius of the needle. Diffusivity is best obtained by fitting the temperatures measured a fixed distance (the KD2 Pro uses 6 mm) from the heated needle (k is also determined from these data). Volumetric specific heat (W/m³ K) is determined from k and D:

$$C = k/D$$

In each case, k and D are obtained by a non-linear least squares procedure (Marquardt, 1963), which searches for values of k and D, which minimise the difference between modelled and measured sensor temperatures. Most experiments will not occur under constant temperature conditions. An additional linear drift factor is included in the inverse procedure. This reduces errors substantially.

(Kluitenberg, et al., 1996) give solutions for pulsed cylindrical sources that are not ideal line heat sources. For a heated cylindrical source of radius a (m) and length 2b (m), with temperature measured at its centre, the temperature rise during heating (zero < t ≤ t₁) is:

$$\Delta T = \frac{q}{4\pi k} \int_{r^2/4Dt}^{\infty} U^{-1} \exp(-U) \exp[-(a/r)^2 U] I_0(2au/r) \operatorname{erf}\left(\frac{b}{r} \sqrt{U}\right) du$$



$$\Delta T = \frac{q}{4\pi k} \int_{r^2/4Dt}^{r^2/4D(t-t_1)} U^{-1} \exp(-U) \exp[-(a/r)^2 U] I_0(2au/r) \operatorname{erf}\left(\frac{b}{r} \sqrt{u}\right) du$$

It is important to determine the depth of soil cover, the type of soil or rock and the ground temperature. The depth of soil cover may determine the possible configuration of the ground coil. If bedrock is within 1.5 m of the surface or there are large boulders, it may not be possible to install a horizontal ground loop. For a vertical borehole the depth of soil will influence the cost as, in general, it is more expensive and time consuming to drill through overburden than rock as the borehole has to be cased.

The temperature difference between the ground and the fluid in the ground heat exchanger drives the heat transfer so it is important to determine the ground temperature. At depths of less than 2 m, the ground temperature will show marked seasonal variation above and below the annual average air temperature. As the depth increases the seasonal swing in temperature is reduced and the maximum and minimum soil temperatures begin to lag the temperature at the surface. At a depth of about 1.5 m, the time lag is approximately one month. Below 10 m the ground temperature remains effectively constant at approximately the annual average air temperature (i.e., between 10°C and 14°C in the UK depending on local geology and soil conditions). The annual variation in ground temperatures at a depth of 1.7 m compared to the daily average air temperature measured at the site. It also shows the ground temperature at a depth of 75 m. Drainage plays an important role to improve soil quality in agriculture (HEEP, 2011; HEEP, 2012; HEEP, 2013; HEEP, 2014).



Figure 15. KD2 Pro thermal properties analyser.

$I_0(x)$ represents a modified Bessel function of order zero, $\operatorname{erf}(x)$ is the error function and u is an integration variable. As pointed out by Kluitenberg et al. [34], $\exp[-(a/r)^2 u] I_0(2au/r)$ approaches unity as a/r approaches zero, and $\operatorname{erf}\left(\frac{b}{r} \sqrt{u}\right)$ approaches unity as b/r approaches infinity, reducing Eqs. (14 and 15) to Eqs.(11 and 12).



Figure 16. Data storage device.

4.5. Ground Characteristics



Figure 17. Handheld controller and sensors.



Figure 18. Single-needle sensors for thermal conductivity and resistivity measurements (6 cm) for liquids.



Figure 19. Extended single-needle sensors for thermal conductivity and resistivity measurements (10 cm) for use in hard materials.



Figure 20. Dual-needle sensors for volumetric specific heat capacity and diffusivity measurements (30 mm).

In order to determine the length of heat exchanger needed to meet a given load the thermal properties of the ground will be needed. The most important difference is between soil and rock as rocks have significantly higher values for thermal conductivity. The moisture content of the soil also has a significant effect as dry loose soil traps air and has a lower thermal conductivity than moist packed soil. Low-conductivity soil may require as much as 50% more collector loop than highly conductive soil. Water movement across a particular site will also have a significant impact on heat transfer through the ground and can result in a smaller ground heat exchanger.

The ground temperature is important, as it is the difference between this and the temperature of the fluid circulating in the heat exchanger that drives the heat transfer. At depths of less than 2 m, the ground temperature will show marked seasonal variation above and below the annual average air temperature. As the depth increases, the seasonal swing in temperature reduces and the maximum and minimum soil temperatures begin to lag the temperatures at the surface (e.g., a time lag of approximately one month at 1.5 m, two months at 4 m). The two rock/soil properties that most affect the design of a heat pump system are the thermal conductivity (k) and the thermal diffusivity (D). The thermal properties of common ground types are given in Table 1. The most important difference is between soil and rock because rocks have significantly higher values for thermal conductivity and diffusivity.



Table 1. Typical thermal properties of soil

Material	Conductivity (Wm ⁻¹ K ⁻¹)	Specific heat (kJkg ⁻¹ K ⁻¹)	Density (kgm ⁻³)	Diffusivity (m ² d ⁻¹)
Granite	2.1-4.5	0.84	2640	0.078-
Limestone	1.4-5.2	0.88	2480	0.18
Marble	2.1-5.5	0.80	2560	0.056-
Sandstone	1.4-5.2	0.71	2240	0.084-
Dry	2.1-5.2			0.23
Wet	1.4-1.7	1.3-1.7		0.074-
Clay	1.7-2.4	1.7-1.9	1440-	0.28
Damp			1920	0.11-0.28
Wet		1.3-1.7	1440-	
Sand	2.1-26	1.7-1.9	1920	0.046-
Damp				0.056
Wet*				0.056-
				0.074
				0.037-
				0.046
				0.065-
				0.084

* Water movement will substantially improve thermal properties.

The main consideration with installation of the ground coil is to ensure good long-term thermal contact. Only standard construction equipment is needed to install horizontal ground heat exchanger, i.e., bulldozers or backhoes and chain trenchers. In larger installation in Europe, track type machines have been used to plough in and backfill around the pipe in continuous operation. Drilling is necessary for most vertical heat exchanger installations. The drilling equipment required is

considerably simpler than the conventional equipment for drilling water wells. Drilling methods commonly used are listed in Table 2.

Table 2. Drilling methods for the installation of vertical collectors (Rybach and Sanner, 2000)

Ground	Method	Remarks
Soft, sand	Auger	Sometimes temporary casing required
	Rotary	
Gravel	Auger	Temporary casing or mud additives required
	Rotary	
Soft, silt/clay	Rotary	Usually the best choice
	DTH*	
Medium	Rotary	Temporary casing or mud additives required
	DTH	
Hard	Top hammer	Roller bit, sometimes mud additives required
	DTH	
Very hard	Top hammer	Large compressor required
	ODEX#	
Hard under soft		Special equipment
		In combination with DTH

* Down-the-hole-hammer.

Overburden drilling equipment (Atlas Copco, Sweden).

For the design of thermally efficient and economically sized borehole heat exchanger systems the soil thermal characteristics, especially the thermal conductivity, borehole resistance and undisturbed ground temperature are essential parameters (Table 3). The design and economic feasibility of these systems critically depend upon the estimate of the ground thermal conductivity.

Table 3. Actual values of thermal conductivity



Case number	Simulation duration (hr)	Ground thermal conductivity predicted by numerical model (Austin et al., 2000) (W/m°C)
1	50	1.11
2	50	1.12
3	50	1.26
4	50	1.98
5	50	6.33
6	50	10.51
7	168	1.08
8	168	1.20
9	168	1.66
10	168	3.89
11	168	14.24
12	168	26.14

4.6. Soil Thermal Heat Properties

Based on existing information regarding Sapporo's subsurface geology (using geologic columnar section, etc.), thermal properties (thermal conductivity, heat capacity, etc.) for the soil, which is typically found 0 to 30 m deep underground, were estimated (Table 4).

Table 4. Observed value and estimated value of soil thermal conductivity

Evaluation method	Thermal conductivity (Wm ⁻¹ K ⁻¹)
Observed value by thermo response test	1.37
Estimation value by geologic columnar section	1.27

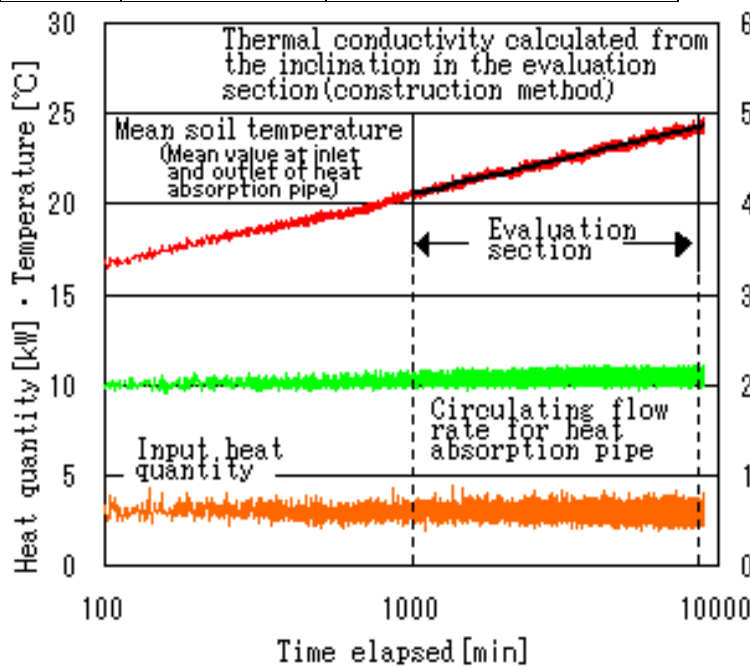


Figure 21. Thermo response test.

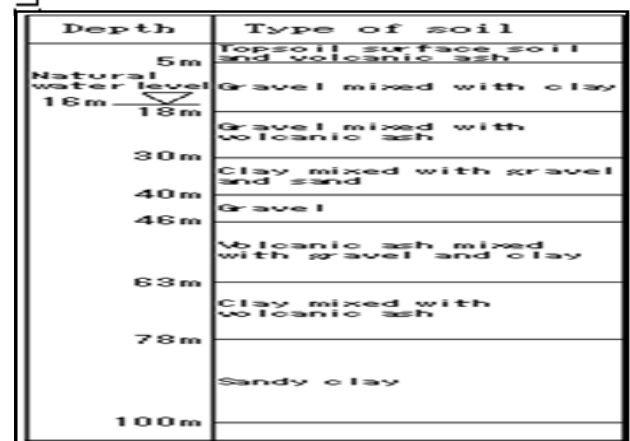


Figure 22. Geologic columnar sections.

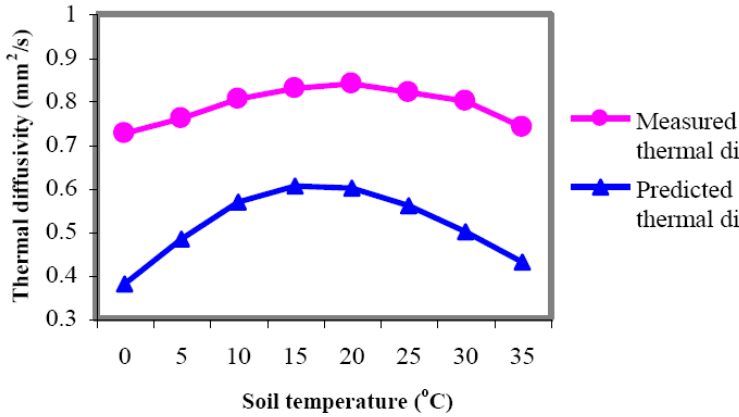


Figure 23. Measured and predicted data of the soil thermal diffusivity.

4.7. Test of Soil Thermal Conductivity

The sample soil thermal conductivity-measuring instrument was produced to measure the soil thermal conductivity from rises in underground temperature (Figure 21). Thermo response test when a certain amount of heat was conducted into heat absorption soil.

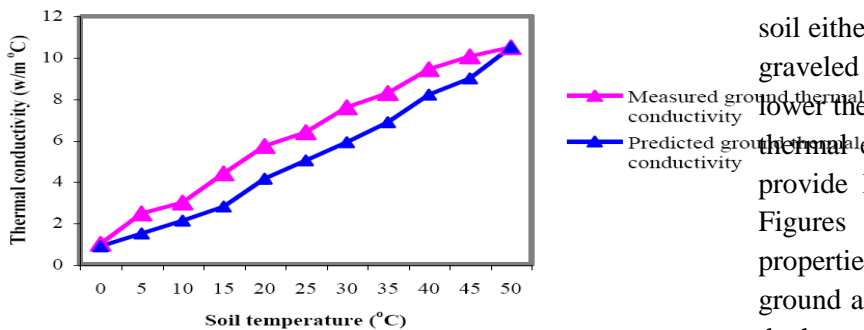


Figure 24. Measured and predicted data of soil thermal conductivity.

According to the measurement result (Table 4), the soil thermal conductivity was observed slightly higher than the thermal conductivity estimated by the geologic columnar section (Figure 22). The future plan is to predict system operational performance at each observation point, based on the relationship between estimated soil thermal property and measured soil thermal conductivity.

Figures 23-24 show the examples of measured and predicted soil temperatures.

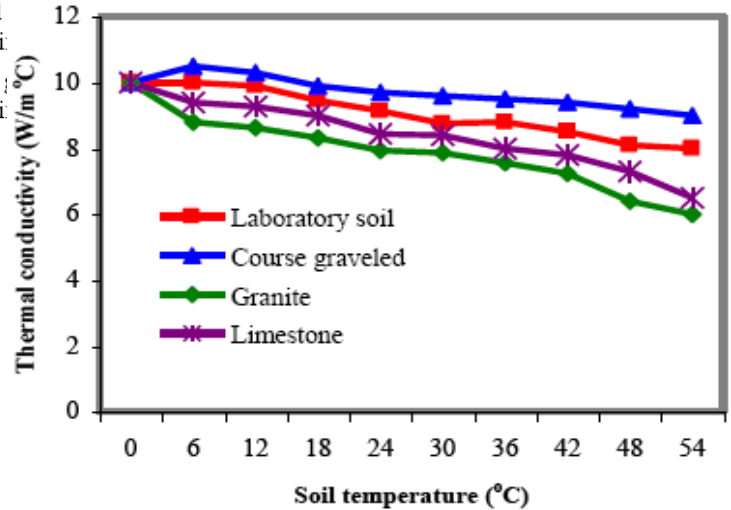


Figure 25. Comparison of thermal conductivity for different soils.

It is seen from the figures that temperature drops much faster for granite and slower for the coarse graveled soil either in the soil. This is mainly due to the fact coarse graveled material has a higher thermal storage capacity or lower thermal diffusivity than granite. Therefore, the high thermal energy stored found in the coarse graveled can provide longer heat extraction as shown in Figure 25. Figures 26-29 show summary of the soil thermal properties. The temperature difference between the ground and the fluid in the ground heat exchanger drives the heat transfer so it is important to determine the ground temperature. At depths of less than 2 m, the ground temperature will show marked seasonal variation above and below the annual average air temperature. As the depth increases the seasonal swing in temperature is reduced and the maximum and minimum soil temperatures begin to lag the temperature at the surface. At a depth of about 1.5 m, the time lag is approximately one month. Below 10 m the ground temperature remains effectively constant at approximately the annual average



air temperature (i.e., between 10°C and 14°C depending on local geology and soil conditions). The annual variation in ground temperatures at a depth of 1.7 m compared to the daily average air temperature measured at the site. It also shows the ground temperature at a depth of 75 m.

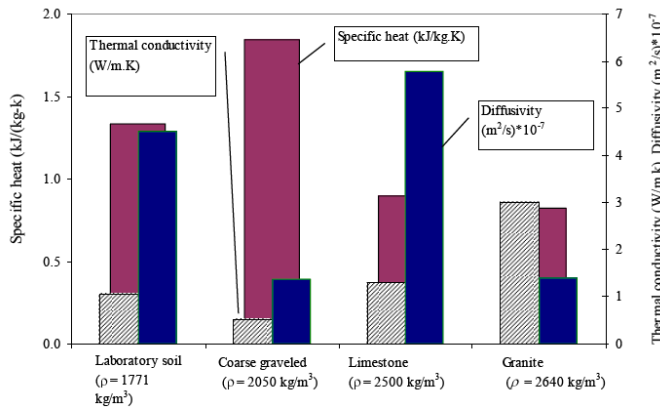


Figure 26. Thermal properties for different soils.

4.8. Ground Temperature

The temperature difference between the ground and the circulating fluid in the heat exchanger drives the heat transfer. So it is important to know the ground temperature. Figure 30 shows the profile of soil temperature. As the depth increases the seasonal swing in temperature is reduced and the maximum and minimum soil temperatures begin to lag the temperatures at the surface. An empirical formula suggested by (Eggen, 1990) is:

$$T_m = T_o + 0.02$$

where:

T_m is the mean ground temperature (°C)

T_o is the annual mean air temperature (°C)

H is the depth below the ground surface (m)

The temperature variation disappears at lower depth and below 10 m the temperature remains effectively constant at approximately the annual mean air temperature.

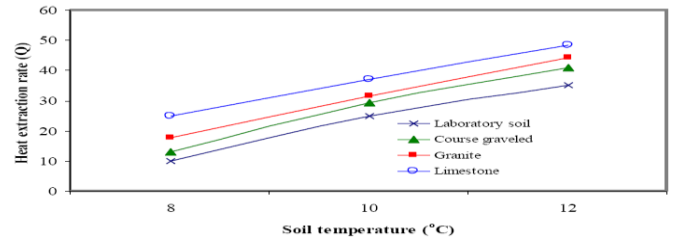


Figure 27. Heat extraction rate for 4 types of soils.

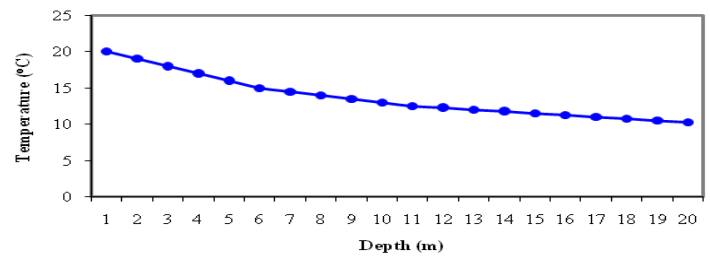


Figure 28. Variation of soil temperature ground depth.

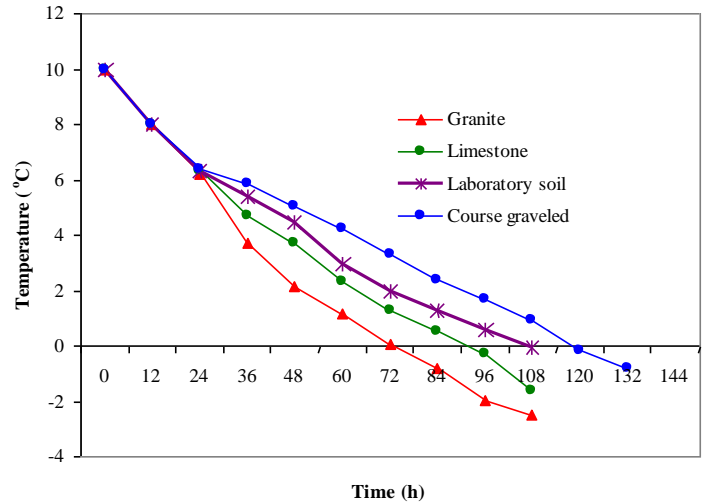


Figure 29. Effect of soil properties on ground water temperatures.

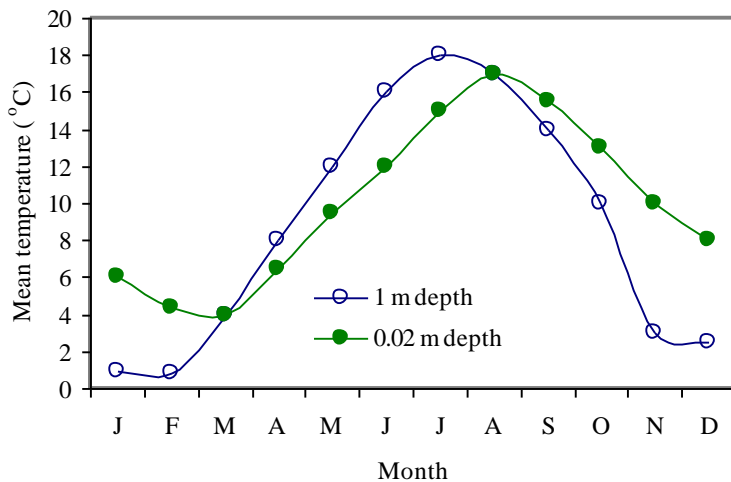


Figure 30. Seasonal variation of soil temperature at depths of 0.02 m and 1 m.

It is important to maximise the efficiency of a heat pump when providing heating, not only to have a low heating distribution temperature but also to have as high a source temperature as possible. Overall efficiencies for the GSHPs are inherently higher than for air source heat pumps because ground temperatures are higher than the mean air temperature in winter and lower than the mean air temperature in summer. The ground temperature also remains relatively stable allowing the heat pump to operate close to its optimal design point whereas air temperatures vary both throughout the day and seasonally and are lowest at times of peak heating demand. For heat pumps using ambient air as the source, the evaporator coil is also likely to need defrosting at low temperatures. It is important to determine the depth of soil cover, the type of soil or rock and the ground temperature. The depth of soil cover may determine the possible configuration of the ground coil. In order to determine the length of heat exchanger needed to meet a given load the thermal properties of the ground will be needed. The most important difference is between soil and rock as rocks have significantly higher values for thermal conductivity (Table 5). The moisture content of the soil also has a significant effect as dry loose soil traps air and has a

lower thermal conductivity than moist packed soil. Low-conductivity soil may require as much as 50% more collector loop than highly conductive soil. Water movement across a particular site will also have a significant impact on heat transfer through the ground and can result in a smaller ground heat exchanger.

Table 5. Peclet numbers corresponding to typical values of thermal properties of soils and rocks

Porous medium	Peclet number $L = a$ typical borehole spacing of (4.5 m)
Soil	
Gravel	5.72E+02
Sand (coarse)	1.34E+01
Sand (fine)	1.15E+00
Silt	1.28E-02
Clay	3.2E-05
Rocks	
Limestone, Dolomite	5.92E-03
Karst limestone	5.28E+00
Sandstone	1.77E-03
Shale	1.05E-06
Fractured igneous and metamorphic	6.32E-02
Unfractured igneous and metamorphic	1.00E-07

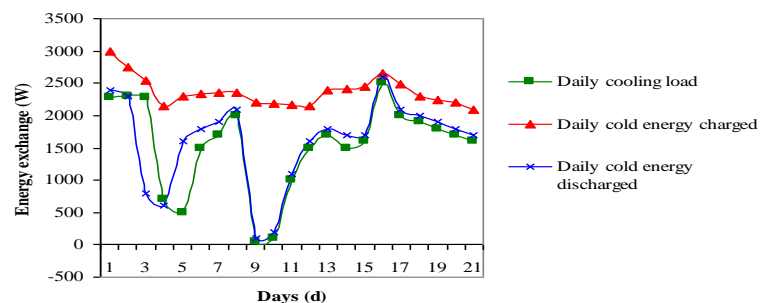


Figure 31. Simulation results in summer.



The thermal and physical properties of soil and its temperature at the far-field boundary remained constant. Heat transfer between a GSHP and its surrounding soil illustrated in Figure 31, which shows the daily cold energy charged to and discharged from its surrounding soil using DX-GSHP at different days. The daily cold energy charged in the initial pre-cooling period sharply decreased, while during the normal operating period, it increased gradually, and the building cooling load although is not big. The net energy exchange in the soil after one year of operation was only 3% of the total cold energy charged, which solved the soil temperature changing acutely to some extent after the yearly operation of the GSHP. The system is feasible technically and the operation mode is reasonable.

5. DISCUSSIONS

Refrigerants are present in GSHP systems and so present the threat of HCFCs and toxicity. However, new types and blends of refrigerant (some using CO₂) with minimal negative impacts are approaching the market as shown in Table 6. Because GSHPs raise the temperature to around 40° they are most suitable for underfloor heating systems or low-temperature radiators, which require temperatures of between 30° and 35°. Higher outputs, such as to conventional radiators requiring higher temperatures of around 60° to 80° can be obtained through use of the GSHP in combination with a conventional boiler or immersion heater.

5.1. Initial Cost

The initial cost of a geothermal heat pump system varies greatly according to local labour rates, geological profile, type of system installed, and equipment selected. The initial cost of GHP systems does come at a premium when compared to air source heat pump systems. For either system, the cost of installed ducts should be identical. Equipment costs can be 50-100% more expensive for a GHP system when the circulating pump, indoor tubing, and water source heat pump are

considered. This 50-100% premium translates to \$1000 - \$2000 for a 3-ton system.

The ground loop is generally the most expensive component of a geothermal heat pump system and is highly dependent on local labour rates and drilling conditions. An installed ground loop stubbed out in a home can run between \$1000 and \$3000 per installed ton. Overall, one could expect to pay between \$4000 and \$11000 more for a turnkey 3 ton GSHP system than for an air source heat pump system. Many consumers justify this initial investment with the savings they expect to realise on their heating and cooling bills over time.

Table 6. CO₂ emissions

System	Primary Energy Efficiency (%)	CO ₂ emissions (kg CO ₂ /kWh heat)
Oil fired boiler	60 – 65	0.45 – 0.48
Gas fired boiler	70 – 80	0.26 – 0.31
Condensing gas boiler	100	0.21
+ low temperature system	36	0.9
Electrical heating		
Conventional electricity + GHSP	120-160	0.20-0.27
Green electricity + GHSP	300-400	0.00

The most formidable barrier to the GSHP systems is currently high installation costs. While this is especially true in the residential sector, it also applies to commercial applications. Residential premiums compared to a standard electric cooling/natural gas heating system (9.0 SEER, 65% AFUE) are typically \$600 to \$800 per ton for horizontal systems and \$800 to \$1000 per ton for vertical systems. Simple payback is typically five to eight years.



The percent increase is somewhat less for commercial GSHPs as shown in the following section.

5.2. Projected Cost of Commercial GSHPs

The cost of vertical ground coil ranges between (\$2.00 to \$5.00) per ft of bore. Required bore lengths range between 125 ft per ton for cold climate, high internal load, and commercial buildings to 250 ft per ton for warm climate installations. Pipe cost can be as low as \$0.20 per ft of bore (\$.10/ft of pipe) for 3/4 inch (2.0 cm) and as high as \$1.00 per ft of bore (\$0.50/ft of pipe) for 1½ inch (4.0 cm) polyethylene pipe. Drilling costs range from less than \$1.00 per ft to as high as \$12.00 per ft. However, \$5.00 per ft is typically the upper limit for a drilling rig designed for the small diameter holes required for the GSHP bores even in the most difficult conditions. It should be noted that larger diameter pipes result in shorter required bore lengths. Table 7 gives typical costs for low and high drilling cost conditions for 3/4 and 1½ inch U-bends for a 10 ton system.

Table 7. Cost of vertical ground coils

System	\$1.50/ft Drilling cost	\$4.00/ft Drilling cost
	¾’’ (2000’)	1½’’ (1700’)
Drilling	\$3000	\$2550
Pipe	\$600	\$1360
Fittings	\$300	\$300
Total	\$3900	\$4210
Cost/ton	\$390	\$421

The total cost will be in the range of \$400 to \$850 per ton. If the cost of the GSHP boiler, drains, and cooling tower is deducted from the total and the cost of the ground coil and current cost of improved heat pumps (\$100/ton) is added, a cost range for the GSHPs results. This leads to the conclusion that the cost of the GSHPs for low cost drilling sites is actually lower than conventional 2-pipe VAV systems.

5.3. Running Costs

Geothermal heat pumps offer high efficiency and low operating cost. Geothermal heat pumps can save homeowners 30-70 percent on heating and 20-50 percent on cooling costs over conventional systems.

Limited data is available documenting the operating cost of the GSHPs in commercial applications. The steady state and part load cooling efficiencies of vertical GSHPs appear to be superior to high efficiency central systems. The heating efficiencies are very good, especially when the ground coil is sized to meet the cooling requirement. However, these high efficiencies will not be realised if ground coils are undersized or low and moderate efficiency water-to-air heat pumps are used. A comprehensive study of the GSHP operating costs in commercial buildings must be conducted. This study is needed to expand the limited design guidelines currently available for the GSHPs.

High installation costs have been identified as a major barrier to wider application of GSHPs often referred to as geothermal heat pumps. The primary reason cited for higher cost is the ground loop. Other factors may be high costs of GSHP heat pump units and supplies, interior installation, and limited competition.

The average cost of ground-source heat pump systems ranged from \$2,360 per ton (5-ton horizontal) to \$3,000 per ton (3-ton vertical). The costs have been subdivided by components (Figure 32). Figure 33 show the comparison of present values of different energy sources.

- Ground loop = 27.2% to 34.2%
- Heat pump = 27.3% to 30.2%
- Indoor installation = 19.2% to 21.1%
- Ductwork = 13.5% to 14.5%
- Pumps = 6.2% to 6.9%

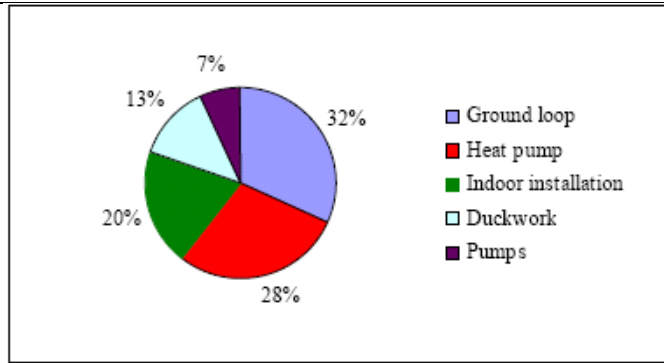


Figure 32. Average cost of the GSHPs.

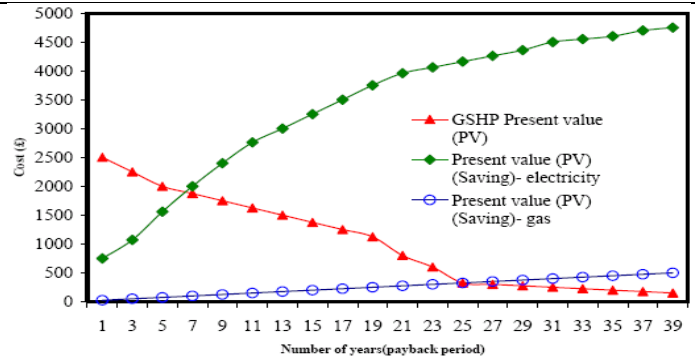


Figure 33. Comparison of present values of different energy sources.

Table 8. Costs and CO2 emissions of the ground source system compared with other alternatives

System	Capital cost installed (£)	Energy consumption (kWh)	Annual running cost (£)	Annual CO ₂ emissions (kgCO ₂)
Ground source heat pump	1800	7825	420	3600
All electric ² (efficiency 100%)		18690	545-1100	8590
Regular oil-fired boiler (efficiency 70%)	1280	26686	380	7210
Regular oil-fired boiler (efficiency 79%)		23646	340	6390
Gas-fired condensing boiler (efficiency 85%)		21976	365	4260

The reasons for these higher costs and lost market opportunities appear to be:

- 1) High cost of ground loops.
- 2) Higher cost for GSHP heat pump equipment and supplies.
- 3) Higher cost of HVAC installation.
- 4) Limited competition.

5.4. Maintaining Soil Fertility and Renewal of Natural

The broad diversity in the soil and multiple in climates from the desert to the tropical climate and refracted number of rivers and included in the rain and a large of groundwater, which led to the diversity and ecological-environmental consequence, in many of the uses and production methods and type crop. Mentors plan focused on a spate irrigation system, lasting and select specific sites in each system are piled cultivation period and provide broad success factors and mixed organic agriculture and surveys to map each region and for the renewal of the characteristics of the site and the quality of crops and the work of initial or renewed tests of the soil to determine the level of organic matter (fertility). The



features of the need to surveys and draw maps of the areas spate irrigation to determine the characteristics of different locations on the level of silting and flooding regularity every year and promote scientific research in the areas of organic agricultural production and provide the necessary funding to encourage companies and agricultural sectors and producers of the founding organic of farms recorded internationally, in addition to the introduction of crop cultivation and promising mandate for such a plant Alhohopa - white sesame – medicinal and aromatic plants -horticultural crops and fodder to the establishment of a central market for crops and vegetables standard specifications and the establishment of villages by the modern complexes of trustees and by the Ministries of Agriculture to follow product quality control and develop and disseminate a culture of total quality and build organic production technologies (SHCP, 2014).

The plan emphasised the important role of agricultural research mandate and urged agricultural research stations on the implementation of research programmes to provide financial and technical support for the draft organic farmers, providing information on soil management techniques and the destruction of organic materials within the plant and animal field and fermentation of organic materials and uses, in addition to information relevant agricultural-related courses fertilises the soil and control weeds and reduce transmission between crop and pests, well as providing technologies for operations aimed at raising agricultural productivity and the means biological control of pests and weeds.

CONCLUSION

In the present work, the effects of sand-bentonite backfill materials on the thermal performance of the BHEs were analysed quantitatively. Laboratory thermal probe tests were conducted to measure the thermal conductivity of sand-bentonite mixtures under different mixed ratios. The mechanism of bentonite affecting heat conduction between the sand grains was revealed from the point of view of microscopic observations. Further,

field tests were carried out to compare the thermal performance of two double U-shaped BHEs with different backfill materials. From the experimental results discussed above, the following conclusions can be obtained:

- 1) The thermal conductivity of sand-bentonite mixtures first increases with increasing percentage of bentonite by dry mass, then reaches a peak at the range from 10% to 12%, beyond which the thermal conductivity decreases quickly. That is to say, for sand-bentonite mixtures used as a backfill material of geothermal boreholes, there exists an optimal percentage of bentonite by dry mass, i.e., 10-12%. If the requirements on the thermal performance of the BHEs are not very strict, an extended range of 8-12% is also acceptable. This extends the results recommended by ASHRAE.
- 2) For the BHE with an optimal sand-bentonite backfill material, the heat injection and heat extraction rate can be enhanced on average by 31.1% and 22.2%, respectively, compared with the case with a common sand-clay material. The present results can provide helpful guides for the design of the GSHP systems.

REFERENCES

- Abdeen M. Omer, Energy use and environmental: impacts: a general review, *Journal of Renewable and Sustainable Energy*, Vol.1, No.053101, 1-29, United State of America, September 2009.
- Abdeen M. Omer, Sustainable energy development and environment, *Research Journal of Environmental and Earth Sciences*, Vol.2, No.2, 55-75, Maxwell Scientific Organisation, Pakistan, April 20, 2010.
- Abdeen M. Omer, Towards the development of green energy saving mechanisms, *Journal of Horticulture and Forestry*, Vol.2, No.7, 135-153, Nigeria, July 2010.



- Abdeen M. Omer, et al. Performance and potential applications of direct expansion ground source heat pump systems for building energy, *Journal of Energy and Power Engineering*, Vol.4, No.1, 1-12, USA, March 2011.
- Abdeen M. Omer, Ventilation and indoor air quality, *Cooling India Magazine*, Vol.7, No.12, 50-57, India, March 2012.
- Abdeen M. Omer, Ground source heat pump technology advancements in buildings, *Cooling India Magazine*, Vol.8, No.1, 80-91, India, 2012.
- Abdeen M. Omer, Chapter 1: Geothermal energy systems, technology, geology, greenhouse gases and environmental pollution control, In: *Geothermal Energy, Technology and Geology*, Editors: J. Yang, 1-45, NOVA Science Publishers, Inc., New York, USA, 2012.
- Abramowitz, M; Stegun, IA. Handbook of mathematical functions. Dover Publications, Inc., New York. 1972.
- Allan, ML. Materials Characterisation of Superplasticised Cement–Sand Grout, *Cement and Concrete Research*, vol.30, no.6, 937-942, 2000.
- Allan, M; Kavanaugh, S. Thermal Conductivity of Cementitious Grouts and Impact on Heat Exchanger Length Design for Ground Source Heat Pumps, *International Journal of HVAC&R Research*, Vol. 5, no.2, 87-98, 1999.
- ASHRAE, Handbook of HVAC Applications, Atlanta: American Society of Heating, Refrigerating and Air-Conditioning Engineers, Inc., 2007.
- Austin, WA; Yavuzturk, C; Spitler, JD. Development of an in situ system and analysis procedure for measuring ground thermal properties. *ASHRAE Transactions*, 106 (1): 2-9. 2000.
- Bristow, K., White, R., and Kluitenberg, J., Comparison of Single and Dual-probes for Measuring Soil Thermal Properties with Transient Heating, *Australian Journal of Soil Research*, vol.32, no.3, 447-464, 1994.
- Carslaw, HS; Jaeger, JC. Conduction of heat in solids. 2nd Edition. Oxford.1959.
- Carslaw, H; Jaeger, J. Conduction of Heat in Solids, 2nd Ed., 58-60, Oxford Press, Oxford, 1964.
- Chehaba, G; Moore, D. Parametric Study Examining the Short and Long Term Response of high-density polyethylene (HDPE) Pipes when Installed by Horizontal Directional Drilling, *Tunnelling and Underground Space Technology*, vol.25, no.6, 782-794, 2010.
- Cote, J; Konrad, J. A Generalized Thermal Conductivity Model for Soils and Construction Materials, *Canadian Geotechnical Journal*, vol.42, no.2, 443-458, 2005.
- Darcy, HP. Les fontaines de la Ville de Dijon. Paris. 1856.
- Eggen, G. Ground temperature measurements. Oslo. 1990.
- Engelhardt, I; Finsterle, S. Thermal-hydraulic Experiments with Bentonite/crushed Rock Mixtures and Estimation of Effective Parameters by Inverse Modelling, *Applied Clay Science*, vol. 23, no.1, 111-120, 2003.
- Fetter, CW. Applied Hydrogeology, Charles E. Merrill Publishing Co., Columbus, Ohio, p.488. 1980.
- Fetter, CW. Determination of the direction of groundwater flow. *Ground Water Monitoring Review*, No. 3, 28-31. 1981.
- Freeze, RA; Cherry, A. Guest Editorial — What Has Gone Wrong? *Ground Water*, volume 27, No. 4, July- August 1989.
- Freeze, RA; Cherry, JA. Ground Water, Prentice Hall Inc.; New Jersey. 1979.
- Freeze, RA; Witherspoon, PA. Theoretical analysis of groundwater flow: 2. Effect of water-table configuration and subsurface permeability variation. *Water Resources Research*, Vol. 3, 623-634. 1967.
- Fournier, RO; Potter, RW. Magnesium Correction to the Na-K-Ca Chemical Geothermometer, *Geochim. Cosmochim. Acta*, 43, 1543-1550. 1979.
- Fournier, RO; Rowe, JJ. Estimation of Underground Temperatures from the Silica Content of Water from Hot Springs and Steam Wells. *Am. J. Sci.*, 264, 685-697. 1966.



- Fournier, RO; Truesdell, AH. An Empirical Na-K-Ca Geothermometer for Natural Waters. *Geochim. Cosmochim. Acta*, 37, 1255-1275. 1973.
- Gu, Y; Dennis, L. Modeling the Effect of Backfills on U-tube Ground Coil Performance, *ASHRAE Transactions*, vol.104, no.2, 677-687, 1998.
- Handbook of Environmental Engineering Problems (HEEP). Scrutiny of inflow to the drains applicable for improvement of soil environmental conditions. 2011.
- Handbook of Environmental Engineering Problems (HEEP). Comparison of different drainage systems usable for solution of environmental crises in soil. 2012.
- Handbook of Environmental Engineering Problems (HEEP). Effect of drainage parameters change on amount of drain discharge in subsurface drainage systems. 2013.
- Handbook of Environmental Engineering Problems (HEEP). A comparison between horizontal and vertical drainage systems (include pipe drainage, open ditch drainage, and pumped wells) in anisotropic soils. 2014.
- Hiraiwa, Y., Kasubuchi, T., Temperature Dependence of Thermal Conductivity of Soil over a Wide Range of Temperature (5-75°C), *European Journal of Soil Science*, vol.51, no.2, 211-218, 2000.
- Isiorho, SA; Meyer, JH. The effects of bag type and meter size on seepage meter measurements. *Ground Water*, 37 (3), 411-413. 1999.
- Kluitenberg, GJ; Ham, JM; Bristow, KL. Error analysis of the heat pulse method for measuring soil volumetric heat capacity. *Soil Sci. Soc. Am. J.* 57, 1444-1451. 1996.
- Lu, S; Ren, T; Gong, Y. An Improved Model for Predicting Soil Thermal Conductivity from Water Content at Room Temperature, *Soil Science Society of America Journal*, vol.71, no.1, 8-14, 2007.
- Marquardt, DW. An algorithm for least-squares estimation of nonlinear parameters. *J. Soc. Industrial Application Math.* 11, 431-441. 1963.
- Li, X; Chen, Y; Chen, Z; Zhao, J. Thermal Performances of Different Types of Underground Heat Exchangers, *Energy and Buildings*, vol.38, no.5,543-547, 2006.
- Nidal, H; Randall, C. Soil Thermal Conductivity: Effects of Density, Moisture, Salt Concentration and Organic Matter, *Soil Science Society of America Journal*, vol.64, no.7-8, 1285-1290, 2000.
- Ochsner, TE; Horton, R; Ren, T. A New Perspective on Soil Thermal Properties, *Soil Science Society of America Journal*, vol.65, no.11-12, 1641-1647, 2001.
- Omer, A. Ground Source Heat Pump Systems and Applications, *Renewable and Sustainable Energy Reviews*, vol.12, no.2, 344-371, 2008.
- Qi, C; Wang, H; Wang, E. Experimental Comparison on the Performance of Geothermal Heat Exchangers under Different Backfilled Materials, *Journal of Heating, Ventilation and Air Conditioning*, vol.40, no.3, 79-82, 2010.
- Rybach and Sanner. Ground-source heat pumps installed in Europe in 1998. 2000.
- SHCP (Soil heat calculator Programme). Evaluation of water lifting devices (pumps) over the centuries worldwide. 2014.
- Sanner, B; Karytsas, C; Mendrinis, D; Rybach, L. Current Status of Ground Source Heat Pumps and Underground Thermal Energy Storage in Europe, *Geothermics*, vol.3, no.2, 579-588, 2003.
- Villar, M; Cuevas, J; Martin, P. Effects of Heat/Water Flow Interaction on Compacted Bentonite: Preliminary Results, *Engineering Geology*, vol.41, no.2,257-267, 1996.
- Waite, W; Gilbert, L; Winters, W. Estimating Thermal Diffusivity and Specific Heat from Needle Probe Thermal Conductivity Data, *Review of Scientific Instruments*, vol.77, no.4, 1-5, 2006.
- Wang, X; Ma, W; Huang, Y; Gong, Y. Experimental Study on Super Absorbent Polymer Mixed with the Original Soil as Backfilled Material in Ground Source Heat Pump System, *Acta*



Energiae Solaris Sinica, vol.28. no.1, 23-27, 2007.

Wang, H; Qi, C; Wang, E. Seasonal Effect on In-Situ Thermal Response Tests for Ground Heat Source Pump. *Journal of Heating, Ventilation and Air Conditioning*, vol.39, no.2, 14-18, 2008.

Wang, H; Liu, L; Qi, C. Comparisons of Test Methods to Determine the Ground Thermal Conductivity for

Geothermal Applications, *Transactions of Geothermal Resources Council*, vol.34, no.1, 532-535, 2010.

Wang, H; Qi, C; Gu, J; Du, H. Thermal Performance of Borehole Heat Exchanger under Groundwater Flow: A Case Study from Baoding, *Energy and Buildings*, vol.41, no.12, 1368-1373, 2009.